Ocean Sci. Discuss., 9, 1–24, 2012
www.ocean-sci-discuss.net/9/1/2012/
doi:10.5194/osd-9-1-2012


Ocean Science Discussions



# Interannual coherent variability of SSTA and SSHA in the Tropical Indian Ocean

**J. Q. Feng**[1,2]

[1]Institute of Oceanology, Chinese Academy of Sciences, Qingdao, 266071, China
[2]Key Laboratory of Ocean Circulation and Wave Studies, Chinese Academy of Sciences, Qingdao, 266071, China

Received: 13 December 2011 – Accepted: 13 December 2011 – Published: 4 January 2012

Correspondence to: J. Q. Feng (fengjunqiao@qdio.ac.cn)

Published by Copernicus Publications on behalf of the European Geosciences Union.

## Abstract

Sea surface height derived from the multiple ocean satellite altimeter missions (TOPEX/Poseidon, Jason-1, ERS, Envisat et al.) and sea surface temperature from National Centers for Environmental Prediction (NCEP) over 1993–2008 are analyzed to investigate the coherent patterns between the interannual variability of the sea surface and subsurface in the Tropical Indian Ocean, by jointly adopting Singular Value Decomposition (SVD) and Extended Associate Pattern Analysis (EAPA) methods. Results show that there are two dominant coherent modes with the nearly same main period of about 3–5 yr, accounting for 86 % of the total covariance in all, but 90° phase difference between them. The primary pattern is characterized by a east-west dipole mode associated with the mature phase of ENSO, and the second presents a sandwich mode having one sign anomalies along Sumatra-Java coast and northeast of Madagascar, whilst an opposite sign between the two regions. The robust correlations of the sea surface height anomaly (SSHA) with sea surface temperature anomaly (SSTA) in the leading modes indicate a strong interaction between them, though the highest correlation coefficient appears with a time lag. And there may be some physical significance with respect to ocean dynamics implied in SSHA variability. Analyzing results show that the features of oceanic waves with basin scale, of which the Rossby wave is prominent, are apparent in the dominant modes. It is further demonstrated from the EAPA that the equatorial eastward Kelvin wave and off-equatorial westward Rossby wave as well as their reflection in the east and west boundary, respectively, are important dynamic mechanisms in the evolution of the two leading coherent patterns. Results of the present study suggest that the upper ocean thermal variations on the timescale of interannual coherent with the ocean dynamics in spatial structure and temporal evolution are mainly attributed to the ocean waves.





OSD
9, 1–24, 2012

## 1 Introduction

Sea surface temperature (SST) anomalies and sea surface height (SSH) anomalies are two representative indictors of the variation in the air-sea coupled system. Striking correlations between them have been reported recently (Leuliette et al., 1999). On one hand, steric changes in sea level at large scales are dominated by thermal effects, at long wavelengths SST is a reasonable proxy for the thermal content of the mixed layer (Leuliette, 1999). Consequently, it is can be considered that variation of SST can induce SSHA variability. On the other hand, on the interannual or longer timescales a substantial fraction of the memory of the climate system must reside in the ocean (Leeuwenburgh et al., 2001), so knowing how the ocean interior communicates with SST is important in climate research. In the early years, scientists believed that effects of subsurface variability under the mixed layer in the ocean on SST were small. However, analysis result of recent sea level data makes people gradually realize that SSH can significantly influence the variation of SST (Leeuwenburgh et al., 2001), which will be the focus in the present paper.

The interannual variations in the Tropical Indian Ocean have received unprecedented interests since the discovery of Indian Ocean Dipole (IOD) by Saji et al. (1999) (Webster et al., 1999; Chao, 2003; Qian et al., 2003; Liu et al., 2006, 2007). The role of the Indian Ocean in the regional and global climate has been examined by several previous investigations (Schott, 2009 and references therein). And the most important finding is that the propagation of oceanic waves plays a significant role among the interannual variations, especially the Rossby wave in the South Tropical Indian Ocean (Xie et al., 2002; Rao et al., 2002; Qian et al., 2003). Chambers et al. (1999) analyzed the Indian Ocean warm events during 1994 and 1997 using the TOPEX/Poseidon data, and found that these warm events were resulted in the wind forced Rossby waves associated with the ENSO events, consistent with the results reported by Murtugudde (2000).

The observation facts of Rossby wave in the previous studies are all based on the sea surface height anomalies (SSHA), heat content in the upper ocean levels or depth





OSD

9, 1–24, 2012

of 20° isotherm that represent the density disturbance in the thermocline layer caused by it. Given that Rossby waves involve a perturbation to the density profile of the water column, and that temperature is an important parameter affecting density, it seems plausible that Rossby waves should have a thermal signature. Whether the Rossby wave signature will be detected in the SST or not lies in the extent to which the surface and subsurface fields are coupled, if the SST gradient can be regarded as a proxy for the surface density gradient, and if this surface density gradient is correlated with the density gradient at depth, then perturbations in the density field should also be visible as perturbations in the SST field, hence, it may be possible to observe baroclinic Rossby waves, through their effect on SST (Cipollini, 1997). Hill et al. (2000) have analyzed the global SST data set to measure the phase speed of the Rossby wave for the first time, assuming that the SST record can tell about all the Rossby wave activity.

Thus, it is significant to recognize the Rossby wave signature in the SST as well as its relationship with the dynamic processes on understanding the interannual variability in the Tropical Indian Ocean. However, due to the lack of observations in the past, related study has been seldom in the literatures. Therefore, in the present study we will examine the coherent variability in the Indian Ocean by mainly carrying out SVD and EAPA to SSHA and SSTA, considering the 16 yr of overlap (1993–2008) between the Altimeters missions and the recently released global SST from NCEP, and the role of oceanic waves, especially the Rossby wave. This study provides a new insight on the correlation between coherent changes of interannual sea level and SST.

The organization of the remainder of the paper is as follows. The data and methods are described in the following Sect. 2. The coherent patterns between SSHA and SSTA will be displayed in Sect. 3, the relationship between the leading modes as well as the role of oceanic waves is also discussed in this section. Section 4 presents the summary of this paper.





OSD
9, 1–24, 2012

## 2 Data and methods

We utilized gridded maps of sea level anomaly data over the global ocean for sixteen years from January 1993 to December 2008 available from the altimeters of T/P, ERS, Envisat et al., with horizontal resolution of 1° latitude by 1° longitude. The National Centers for Environmental Prediction-National Centers for Atmospheric Research (NCEP-NCAR) reanalysis SST data were available on 1° latitude by 1° longitude grid over the global ocean each month from December 1981 through 2008. As we are interested in the interannual fluctuations, we work with anomalies relative to the seasonal cycle. We used the Niño 3.4 index, derived from the Extended Reconstructed SST, version 3 (ERSST.v3; Smith and Reynolds, 2008) by NOAA, which is averaged over the central-eastern Pacific (5° S–5° N, 170°–120° W).

One of the most efficient ways to isolate the co-variability between two fields is to apply SVD analysis to the fields (Wallace, 1992; Cheng and Dunkerton, 1995; Leuliette, 1999). Unlike EOF analysis, in which the SSHA and SSTA are used separately, SVD is applied to the cross covariance matrix of the two variables. Thus, the results describing the primary coherent mode can not be assumed to represent the primary oscillation mode of variability for each individual field. The dominant modes explaining large fractions of squared covariance, with strong temporal and spatial correlations, are often interpreted in terms of dominant coherent modes of the data vectors. The heterogeneous correlation maps of the left and right fields, which are the correlation coefficient between the time series of the left modes with the right filed and vice versa, not only can provide a measure of coherent between the fields but can represent the causality between them in certain degrees. For normalized input data these heterogeneous correlation maps have the same patterns as the corresponding left and right singular vectors (Bretherton, 1992). The reader should refer to Bretherton (1992) for further details and to Wallace (1992) for examples of the application of the SVD analysis. When the SVD analysis is performed, especially when the temporal dimension is far larger than the spatial, the resulted SVD modes are not always significant in statistic,





OSD
9, 1–24, 2012

hence couldn't be reasonably explained in physical. So, Shen and Lau (1995), Iwasaka (1995) introduced the Monte Carlo technic to test the statistical significance of the SVD modes, Shi (1996) sketchily described the method, which will be also utilized in the present paper.

Associate pattern (or regression distribution) is defined as an optimal field pattern related to the given time series by the least square method, which has been popularly used in climate studies (Zorita et al., 1992; von Storch et al., 1993). However, it can not tell how much itself is correlated to the given time series. Therefore, associate pattern analysis may not be efficient to extract useful information for statistical analyses, especially for longer time lag analyses (Cui et al., 2004a,b, 2005), to solve this problem, Cui et al. (2004a) proposed the EAPA, which has been successfully used by previous studies (Cui et al., 2004a,b,c, 2005; Wu et al., 2005, 2007), the detail of this method is described in Cui (2004a).

## 3 Results

### 3.1 Leading coherent modes

Since we are interested in the associated spatial and temporal response of SSHA and SSTA, SVD analysis is applied to the temporal cross covariance matrix of the two fields. The confidence test based on Monte Carlo technic shows that only the first two modes for each pair of variables are well beyond 95 % significant level. And the covariance is strongly concentrated in the first two modes which isolate large-scale spatial features with interannual periods.

Figure 1 presents the results of the primary SVD modes, which accounts for 72 % of the total covariance. The lead-lag correlation coefficients between the time series of SSTA and SSHA for the first SVD mode displayed in Fig. 1c are high, as clearly shown in Fig. 5a, suggesting the strong mutual action between the two fields. The prominent period of the time series is about 3–5 yr derived from the Wavelet analysis (Fig. 3a).





OSD
9, 1–24, 2012

The spatial structures displayed both in Fig. 1a,b suggest the basin wide scale of coherent variability between subsurface dynamic and sea surface temperature variability in the Tropical Indian Ocean, which are characterized by opposite signs of both SSTA and SSHA in the Western Indian Ocean and that in the Eastern Indian Ocean (called the dipole mode in the following text, with its corresponding time series defined as dipole index). Figure 1d,e shows heterogeneous maps, characterized by two strong correlated regions in each filed resembling the patterns of the spatial modes. According to the theory of SVD, when the time series of the two variables covary consistently, they will be strongly coherent to each other in the regions where the correlation coefficients show the same sign in the heterogeneous maps. Therefore, the regions of the Southeastern Indian Ocean along Sumatra-Java coast and the Southwestern Indian Ocean are two distinct regions with strong interaction between SSH and SST.

The second SVD mode represents 14 % of the total covariance, the lead-lag correlation coefficients illustrated in Fig. 5b between the two time series (Fig. 2c) is significant as compared to the $t$-test confidence level. The dominant period of the time series is about 3–5 yr (Fig. 3b), too, closing to that of the first mode. Figure 2a,b presents the spatial structure of the second mode for the two fields, with positive anomalies confining in Sumatra-Java coast and northeast of Madagascar, negative anomalies regions centered in South-Central Indian Ocean which extends in the northwest-southeast direction (called the sandwich mode hereafter, with its corresponding time series defined as sandwich index). The coherent spatial patterns between the two fields are highly correlated with each other by comparing the heterogeneous maps depicted in Fig. 2d,e, and the feature of large scale oceanic wave is apparent both in the spatial and heterogeneous maps.

The time series in the first mode show strong activities appearing during 1994–1995, 1997–1998, 2002–2003, 2006–2007, coincident with ENSO event which is known as the dominant signal of the interannual variability taking place in the Tropical Pacific Ocean and significantly influencing the global air-sea coupled system (Philander, 1990). So, the question we will address is whether the primary pattern has some





OSD
9, 1–24, 2012

relation to ENSO event or not. To investigate this problem, we have examined the time series of the primary mode and Niño 3.4 index, displayed in Fig. 5. The correlation coefficient between them is as high as 0.86, far exceeding the 99 % confidence level, implying that the primary mode is strongly related to the mature phase of ENSO. The study result of Tiwari (2004) suggests that ENSO is one of an important external factor forcing the interannual SSHA variability (a proxy of subsurface variability) in the Tropical Indian Ocean, which resembles that displayed in the first SVD mode in our present study. Here, it is further proved that the associated interannual SST variability coherent with SSHA over 1993–2008 is still related to ENSO.

### 3.2 Relationship between the two leading modes

Based on the theory of SVD, different SVD modes are orthogonal to and independent on each other. However, it is not the same relation between their corresponding time coefficients. Results of the SVD analysis are intriguing as the first two modes have a similar prominent period, which may reflect certain relationship between them. In order to examine this, we have carried out the lead-lag correlation analysis. The large positive correlations appear when the sandwich mode lags the dipole mode for about nine to eleven months (Fig. 5c), indicating a nearly quadrature phase difference between them. In addition, the cross wavelet analysis between the time expansion coefficients of the first two SVD modes also suggests that, the largest spectral value appears when the two time series have a quadrature phase difference, consisting with the lead-lag correlation analysis. Therefore, from the temporal point of view, the first two leading modes are not isolated.

As having been illustrated in Sect. 3.1, the first two SVD modes both present features of large scale oceanic waves appearing mainly in the South Indian Ocean, whilst relate to ENSO phenomenon. Longitude-time plots of SSTA and SSHA, averaged along the latitudes between 13 and 9° S shown in Fig. 6, vividly exhibit the clear westward propagation signals, which are identified as the Rossby waves, and each warm Rossby wave is coincident with an El Niño event, agreement with some previous studies (Webster,



OSD
9, 1–24, 2012

Interannual coherent variability of SSTA and SSHA in the Tropical Indian Ocean

J. Q. Feng

1999; Chambers et al., 2000). Moreover, it is shown from Fig. 6 that, there is no appreciable phase lag, i.e., SSHA and SSTA signals for each propagating wave are found to be nearly in phase, according with the result of SVD analysis. White (2000) claimed that warm SSTA overlying high SSHA in the Indian Ocean suggests that vertical displacements in the pycnocline associated with Rossby waves play a dominant role in specifying the phase relationship between SSHA and SSTA. Consequently, together with the principia of SVD method, it is reasonable to suppose that the coherent modes between SSTA and SSHA are attributed to the modulation of ocean dynamic mechanisms dominated by Rossby wave. In other words, the interannual variability with 3–5 yr period in the SSTA field coherent with the SSHA is significantly influenced by the propagation of Rossby waves mainly taking place in the thermocline layer. In the following section, we will perform the EAPA to further document the response of SSTA to SSHA, and assess the role of the oceanic waves.

### 3.3 Extended associate patterns

A modal-transition is indicated in the SVD analysis, that is, dipole mode leads sandwich mode by nearly one year as the Western Indian Ocean warms. Intended to further study the causes of the coherent modes and the modal-transition process, EAPA is carried out in this section.

Associate patterns of SSTA and SSHA for fifteen-month lead through twelve-month lag to the dipole index are calculated and the plots are given every 3 months interval in Fig. 7, with the lag month denoted in the African landmass. According to Cui et al. (2004a, 2005) and Wu et al. (2007), taken the dipole index as $X$, SSTA, SSHA field as Y, the correlation coefficients between the dipole mode and the associate mode are more than 0.5 (Fig. 9a), far exceeding 99 % significant confidence level, and the average variances explained by the associate patterns are more than 15 % (Fig. 9b).

Fifteen months before the dipole index peaks, a warm downwelling Rossby wave with center located at the southeast of Tropical Indian Ocean begins to propagate westward with a low phase speed. Twelve months before the peaks, negative anomalies start to develop along Sumatra-Java coast. Six months before the peaks, the warm Rossby wave arrives at the Southwestern Indian Ocean, the dipole patterns both appearing in the SSHA and SSTA field are formed. Thereafter, with several months' development and strengthening while the warm Rossby wave continuing to propagate westward, the peaks of the dipole mode are witnessed right at the zero lag time. So, propagation of the Rossby wave, especially in the off-equatorial South Indian Ocean, is a dominant mechanism of the coupled dipole mode derived from the SVD analysis.

After the peaks of the dipole mode, from three months lag on, negative anomalous signals both in SSH and SST fields start to propagate westward in the form of Rossby wave from the Eastern Indian Ocean with a trend of southward, meanwhile, the positive anomalous signals in the Western Indian Ocean reflect in the west boundary, eastward propagating as oceanic Kelvin waves along the equator, and reach the east boundary three months later. The pattern of the sandwich mode stands out with the time lag for nine months, then, the cold Rossby wave continues propagating westward. Till the twelfth month lag, the loading patterns totally resemble the peaks of the sandwich mode, which is consistent with the result of lead-lag correlation analysis.

Similarly, SSTA and SSHA associate patterns with time lags from minus twelve to zero months with respect to the sandwich mode are plotted on Fig. 8, to more fully assess the physical process of the evolution from the dipole mode to the sandwich mode. It is clear that the correlation coefficients between the sandwich mode and the associate mode are more than 0.7 (Fig. 9c), and the basin-averaged variances explained by the associate patterns exceeds 20 % (Fig. 9d). By comparing Figs. 7 and 8, we can find that the associate patterns with time lags from zero to twelve in reference to the dipole mode are similar to that with time leads from twelve to zero in reference to the sandwich mode. This highly agreement strongly indicates that EAPA indeed describes the spatial and temporal evolution of the coupled mode between SSHA and SSTA as well as the way through which the dipole mode converts to the sandwich mode.





OSD
9, 1–24, 2012

In conclusion, as expected, the EAPA suggests that the lead-lag relation between the two coherent modes of SSHA and SSTA can be understood in a manner of the propagation of the off-equatorial westward Rossby wave and equatorial eastward Kelvin wave, as well as their reflection at the west and east boundaries, respectively. It is interesting to note that, the SSTA and SSHA amplitudes are decaying gradually from the zero to the twelfth month lag suggested in Fig. 7, which is generally consistent with the frequency spectral energy relationships in terms of quantity displayed in Fig. 3, implying the dying of the dipole mode. In addition, what is the most important here is that the interannual thermal variability in the upper ocean exhibits the same features with the large scale ocean dynamics, suggesting the ocean waves are the main mechanism on the response of surface variability to that in the subsurface.

## 4 Conclusions

The present paper studies the coherence variability between SSHA and SSTA in the Tropical Indian Ocean on time scale of interannual over 1993–2008. SVD analysis suggests that there are two dominant coherent patterns between SSHA and SSTA isolating large-scale spatial features with the main period of 3–5 yr, capturing 86 % of the overall covariance. The primary pattern is characterized by the dipole mode strongly related to the mature phase of ENSO, and the second presents a conversion mode with a sandwich pattern, there are 90° phase difference between them. Similar interannual patterns have been also reported by Leuliette et al. (1999) for the first time, who investigated the contribution of the thermal expansion to sea level by using the same SVD analysis between SSTA and SSHA. Here, we mainly focus on the response of SSTA to SSHA associated with ocean dynamics. The equatorial eastward Kelvin waves and off-equatorial westward Rossby waves as well as their reflection in the east and west boundaries, respectively, play an important role on the formation of the dipole mode, and evolution of the sandwich mode. In other words, it is fully indicated that the propagation of oceanic waves is an important mechanism in the variation of SST coherent with the subsurface variability on timescale of interannual.





OSD
9, 1–24, 2012

Strictly speaking, in theory, the response of SSTA to SSHA is not fully simultaneous, and vice versa. It is can be clearly seen from Fig. 5a (Fig. 5b) that the highest correlation coefficient appears at about one month lag of SSHA (SSTA) with respect to SSTA (SSHA) in the first (second) mode. That is to say, a time delay presents between the wave transition suggested in the SSHA field and the adjustment of the SSTA. However, this time lag could be neglected on the timescale we are interested in here, partly because of the characteristics of the fields obtained by SVD analysis, a way through which finding the coherent variability. Moreover, White (2000) also found all three SSHA, SSTA, and MSW (Meridional Surface Wind) interannual variables display significant spectral coherence, with oceanic and atmospheric variability propagating westward in fixed 0° phase with one another, which is unique in the Tropical Indian Ocean. Hence, the adjustment time of SSTA to SSHA is shorter than the timescale of wave motions demonstrated above. Therefore, the result that interannual subsurface variability impacts that in the surface via ocean waves, mainly Rossby wave, is reasonable. Results of the present paper substantiate the fact of the phase relationship between SSHA and SSTA claimed by White (2000) associated with Rossby waves, providing a foundational observation evidence for further studies.

*Acknowledgements.* This work is supported by the Natural Science Foundation of China (41106016).

## References

Bretherton, C. S., Smith, C., and Wallace, J. M.: An intercomparison of methods for finding coupled paterns in climate data, J. Climate, 5, 541–560, 1992.

Chambers, D. P., Tapley, B. D., and Stewart, R. H.: Anomalous warming in the Indian Ocean coincident with El Niño, J. Geophys. Res., 104, 3035–3047, 1999.

Chao, J. P. and Yuan, S. W.: Connection of air-sea interaction between Tropical Indian and Pacific Oceans, Progr. Nat. Sci., 13(12), 1280–1285, 2003, (in Chinese with English abstract).

Cheng, X. and Dunkerton, T. J.: Orthogonal rotation of spatial patterns derived from singular value decomposition analysis, J. Climate, 8, 2631–2643, 1995.





OSD

9, 1–24, 2012

Cipollini, P., Cromwell, D., Jones, M. S., Quartly, G. D., and Challenor, P. G.: Concurrent altimeter and infrared observations of Rossby wave propagation near 34° N in the Northeast Atlantic, Geophys. Res. Lett., 24(8), 889–892, 1997.

Cui, M. C. and Wu, L. J.: El Niño phenomenon in SODA data, Acta Oceanol. Sin., 24(4), 43–53, 2005.

Cui, M. C., Mo, J., and Qiao, F.: El Niño phenomenon and extended associate pattern analysis, J. Hydrodynam., 16B(1), 90–100, 2004a.

Cui, M. C., Hu, D. X., and Mo, J.: Seasonality and causes of the Yellow Sea warm current, Chin. J. Oceanol. Limnol., 22(3), 265–270, 2004b.

Cui, M. C., Hu, D. X., and Wu, L. J.: Seasonal and intraseasonal variations of the surface Taiwan Warm Current, Chin. J. Oceanol. Limnol, 22(3), 271–277, 2004c.

Hill, K. L., Robinson, I. S., and Cipollini, P.: Propagation characteristics of extratropical planetary waves observed in the ATSR global sea surface temperature record, J. Geophys. Res., 105(C9), 21927–21945, 2000.

Iwasaka, N. and Wallace, J. M.: Large scale air sea interaction in the Northern Hemisphere from a view point of variations of surface heat flux by SVD analysis, J. Meteorol. Soc. Jpn., 73(4), 781–794, 1995.

Leeuwenburgh, O. and Stammer, D.: The effect of ocean currents on sea surface temperature anomalies, J. Phys. Oceanogr., 31, 2340–2358, 2001.

Leuliette, E. W. and Wahr, J. M.: Coupled pattern analysis of sea surface temperature and TOPEX/Poseidon sea surface height, J. Phys. Oceanogr., 29, 599–611, 1999.

Li, C. Y. and Mu, M. Q.: The influence of the Indian Ocean dipole on atmospheric circulation and climate, Adv. Atmos. Sci., 18(5), 831–843, 2001 (in Chinese with English abstract).

Liu, L. and Yu, W. D.: Connection between Tropical Indian Ocean dipole event and Subtropical Indian Ocean dipole event, Adv. Mar. Sci., 24(3), 301–306, 2006 (in Chinese with English abstract).

Liu, L. and Yu, W. D.: An analysis of the interannual variability of precipitation in the Tropical Indian Ocean, Periodical of Ocean University of China, 37(1), 15–20, 2007 (in Chinese with English abstract).

Liu, L., Yu, W. D., and Liu, Y. G.: Correlation between interannual Indian Ocean dipole and ENSO, J. Zhanjiang Ocean Univ., 26(3), 50–55, 2006 (in Chinese with English abstract).

Murtugudde, R., McCreary, J. P., and Busalacchi, A. J.: Oceanic processes associated with anomalous events in the Indian Ocean with relevance to 1997–1998, J. Geophys. Res., 105,

3295–3306, 2000.
Philander, S. G. H.: El Niño, La Niña and the Southern Oscillation, Academic Press, New York, 289, 1990.
Qian, W. H., Hu, H. R., and Zhu, Y. F.: Thermocline oscillation and warming event in the Tropical Indian Ocean, Atmosphere-Ocean, 241–258, 2003.
Rao, S. A., Behera, S. K., Masumoto, Y., and Yamagata, T.: Interannual subsurface variability in the Tropical Indian Ocean with a special emphasis on the Indian Ocean dipole, Deep-Sea Res., 49, 1549–1572, 2002.
Saji, N. H. and Yamagata, T.: Possible impacts of Indian Ocean dipole mode events on global climate, Clim. Res., 25, 151–169, 2003.
Saji, N. H., Goswami, B. N., Vinayachandran, P. N., and Yamagata, T.: A dipole mode in the Tropical Indian Ocean, Nature, 401, 360–363, 1999.
Schott, F. A., Xie, S. P., and McCreary, P.: Indian Ocean circulation and climate variability, Rev. Geophys., 47, RG1002, doi:10.1029/2007RG000245, 2009.
Shi, N.: Confidence test of SVD method in the study of Climate Diagnose, Meteorol. Sci. Technol., 4, 5–6, 1996 (in Chinese).
Shen, S. and Lau, K. M.: Biennial oscillation associated with the east asian summer monsoon and tropical sea surface temperatures, J. Meteorol. Soc. Jpn., 73(1), 105–124, 1995.
Smith, T. M., Reynolds, R. W., and Peterson, T. C.: Improvements to NOAA's historical merged land-ocean surface temperature analysis (1880–2006), J. Climate, 21, 2283–2296, 2008.
Tiwari, V. M., Cabanes, C., DoMinh, K., and Cazenave, A.: Correlatin of interannual sea level variations in the Indian Ocean from Topex/Poseidon altimetry, temperature data and tide gauges with ENSO, Global Planet. Change, 43, 183–196, 2004.
Von Storch, H., Zorita, E., and Cubasch, U.: Downscaling of global climate change estimates to regional scales: an application to Iberian rainfall in wintertime, J. Clim. 5, 1161- 1171, 1993.
Wallace, J. M., Smith, C., and Bretherton, C. S.: Singular value decomposition of wintertime sea surface temperature and 500-mb height anomalies, J. Climate, 5, 561–576, 1992.
Webster, P. T., Moore, A. M., Loschning, J. P., and Leben, R. R.: Coupled ocean-atmosphere dynamics in the Indian Ocean during 1997–98, Nature, 401, 356–360, 1999.
White, W. B.: Coupled Rossby waves in the Indian Ocean on interannual timescales, J. Phys. Oceanogr., 30, 2972–2988, 2000.
White, W. B., Ghao, Y., and Tai, C. K.: Coupling of biennial oceanic Rossby waves with the overlying atmosphere in the Pacific basin, J. Phys. Oceanogr., 28, 1236–1251, 1998.

Wu, L. J., and Cui, M. C.: Statistical analysis of surface hydrography and circulation variations in Northern South China Sea, Chin. J. Oceanol. Limnol., 23(4), 383–392, 2005.
Wu, L. J., Wang, F., Yuan, D. L., and Cui, M. C.: Evolution of freshwater plumes and salinity fronts in the Northern Bay of Bengal, J. Geophys. Res., 112, C08017, doi:10.1029/2005JC003308, 2007
Xie, S. P., Annamalai, H., Schott, F., and McCreary, J. P.: Structure and mechanisms of south Indian Ocean climate variability, J. Climate., 15, 864–878, 2002.
Xue, F. and He, J. X.: The influence of the extratropical atmospheric disturbances on ENSO, Chinese J. Geophys., 50(5), 1311–1318, 2007 (in Chinese with English abstract).
Zorita, E., Kharin, V., and von Storch, H.: The atmospheric circulation and sea surface temperature in the North Atlantic area in winter: their interaction and relevance for Iberian precipitation, J. Climate, 5, 1097–1171, 1992.





OSD
9, 1–24, 2012

Interannual coherent variability of SSTA and SSHA in the Tropical Indian Ocean

J. Q. Feng

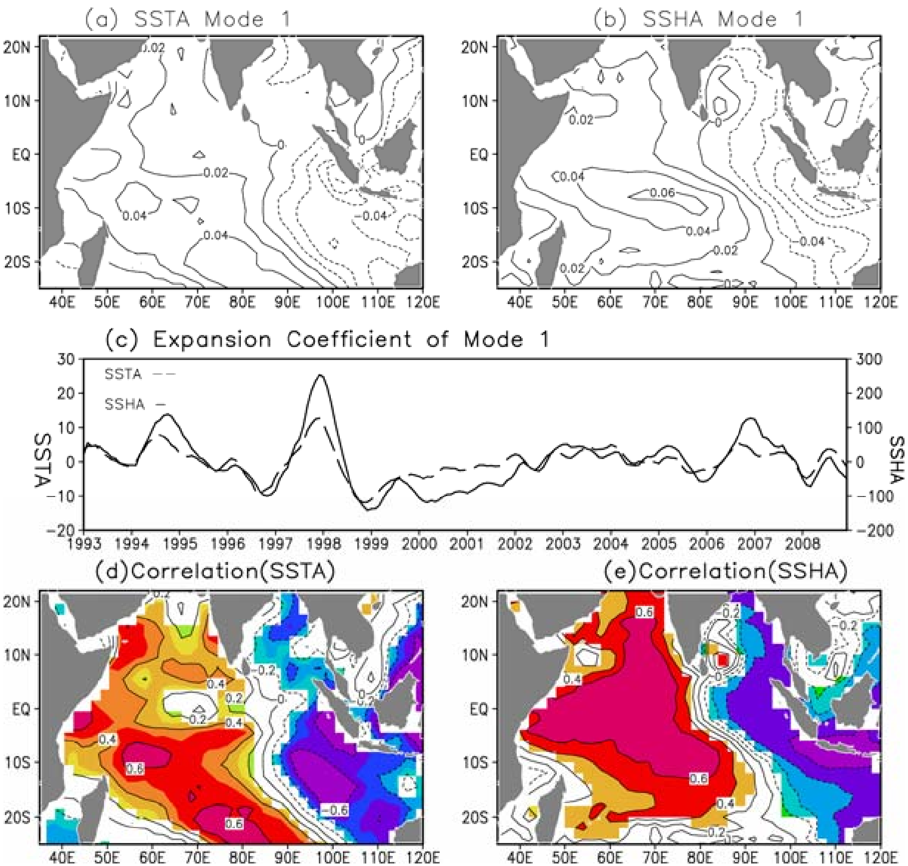


**Fig. 1.** Spatial eigenvectors of SSTA **(a)**, SSHA **(b)** along with their associated eigenfunctions (dashed line denotes SSTA and solid line SSHA) **(c)**, and heterogeneous correlation maps of SSTA **(d)** and SSHA **(e)** for the first SVD mode, with shaded indicating values exceeding 99 % confidence level.





OSD
9, 1–24, 2012

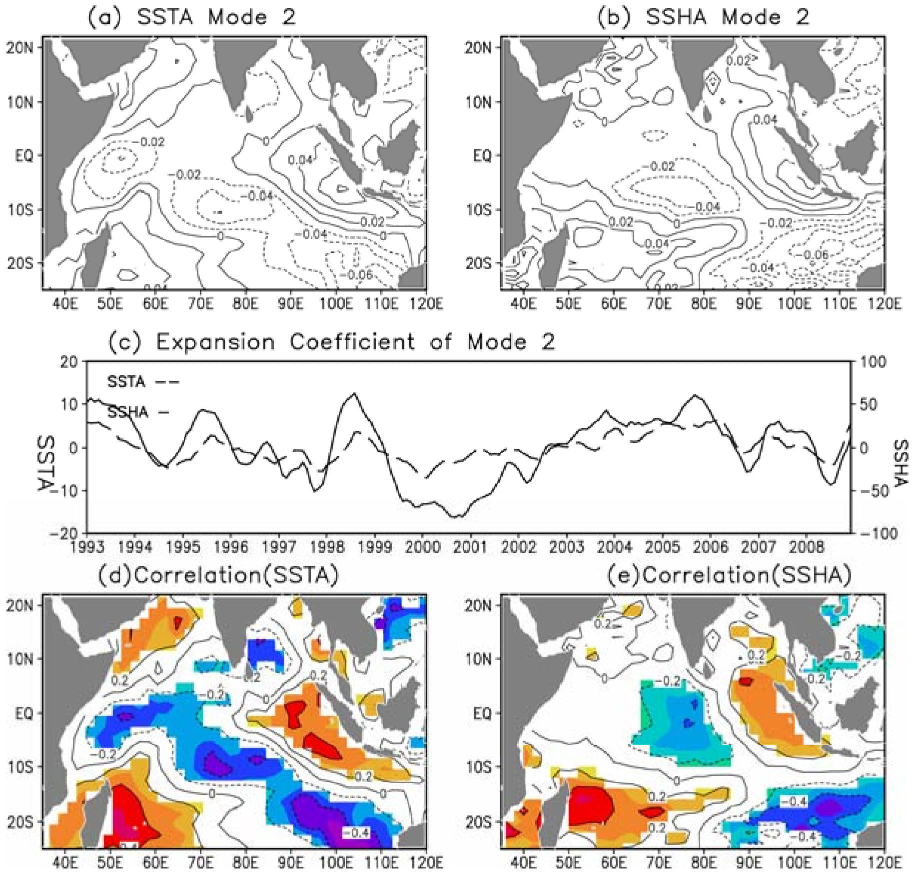


**Fig. 2.** Same as Fig. 1, but for the Second SVD mode.





OSD
9, 1–24, 2012

Interannual coherent variability of SSTA and SSHA in the Tropical Indian Ocean

J. Q. Feng

Title Page
Abstract | Introduction
Conclusions | References
Tables | Figures
◀| |▶
◀ ▶
Back | Close
Full Screen / Esc
Printer-friendly Version
Interactive Discussion

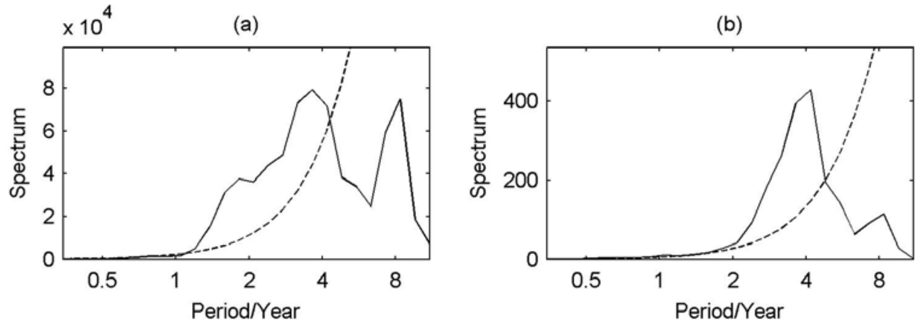


**Fig. 3.** Period-Spectrum plots of time expansion coefficients for the first SVD mode (dipole mode) **(a)** and the second SVD mode (sandwich mode) **(b)**, with dashed lines denoting 95 % confidence level.





OSD
9, 1–24, 2012

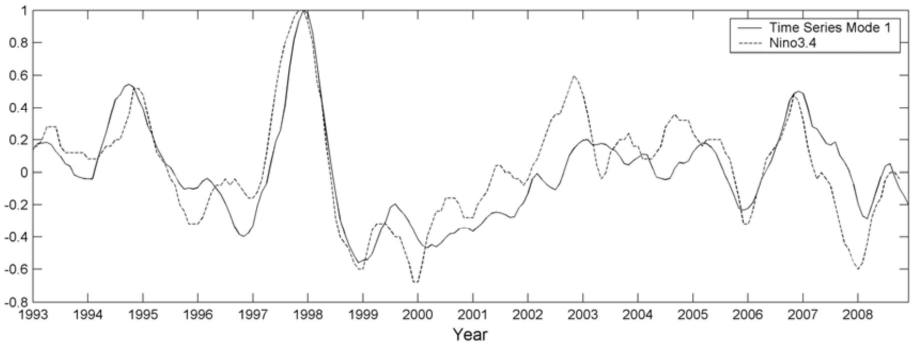


**Fig. 4.** Normalized time expansion coefficients of the first SVD mode for SSHA (solid line) and Niño 3.4 index (dashed line), correlation between them is 0.86, exceeding 99 % confidence level.





OSD
9, 1–24, 2012

Interannual coherent variability of SSTA and SSHA in the Tropical Indian Ocean

J. Q. Feng

Discussion Paper | Discussion Paper | Discussion Paper | Discussion Paper |

OSD

9, 1–24, 2012

Interannual coherent variability of SSTA and SSHA in the Tropical Indian Ocean

J. Q. Feng



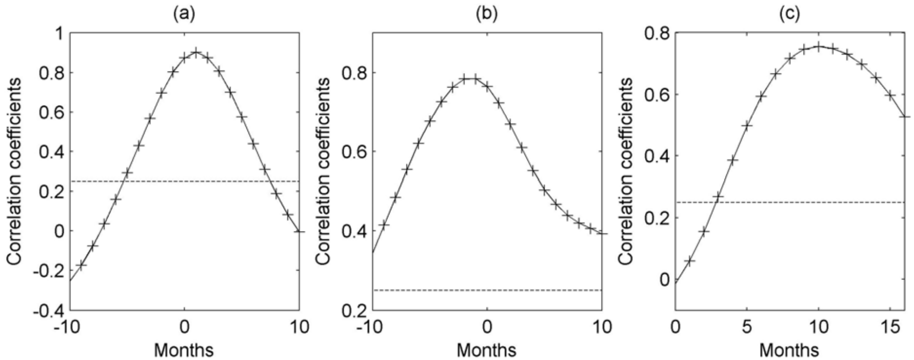


**Fig. 5.** Lag correlation between the temporal coefficients of **(a)** SSHA and SSTA for the first SVD mode, **(b)** SSHA and SSTA for the second SVD modes, **(c)** SSHA for the second SVD mode and SSTA for the first SVD mode, with abscissa presenting lag month. Positive lags denote SSTA leading SSHA in **(a, b)**, while the first leading the second mode in **(c)**. The dashed line is the 99 % confidence level.

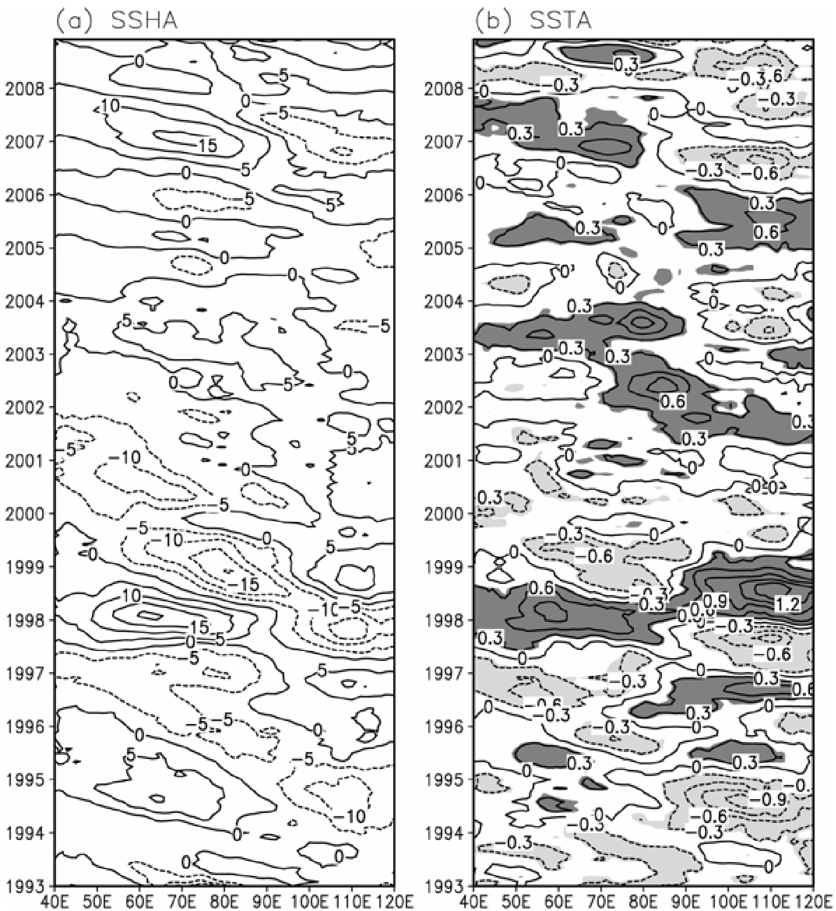


**Fig. 6.** Longitude-time plots of latitude averaged between 13 and 9° S for **(a)** SSHA (unit: cm), **(b)** SSTA (unit: °C)



OSD
9, 1–24, 2012

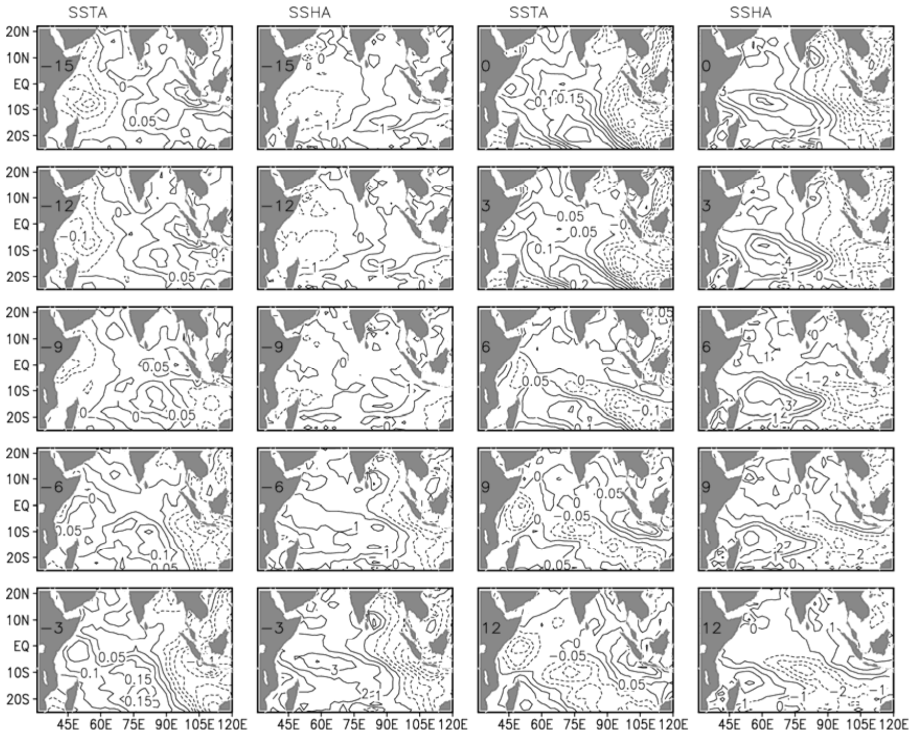


**Fig. 7.** SSTA (the first and the third columns), SSHA (the second and the forth columns) associate patterns with time lags from minus 15 to 12 months in reference to the dipole mode. The lags are every 3 months, as denoted in the African landmass. The units are degree (˚C) and cm for SSTA and SSHA, respectively.





OSD
9, 1–24, 2012

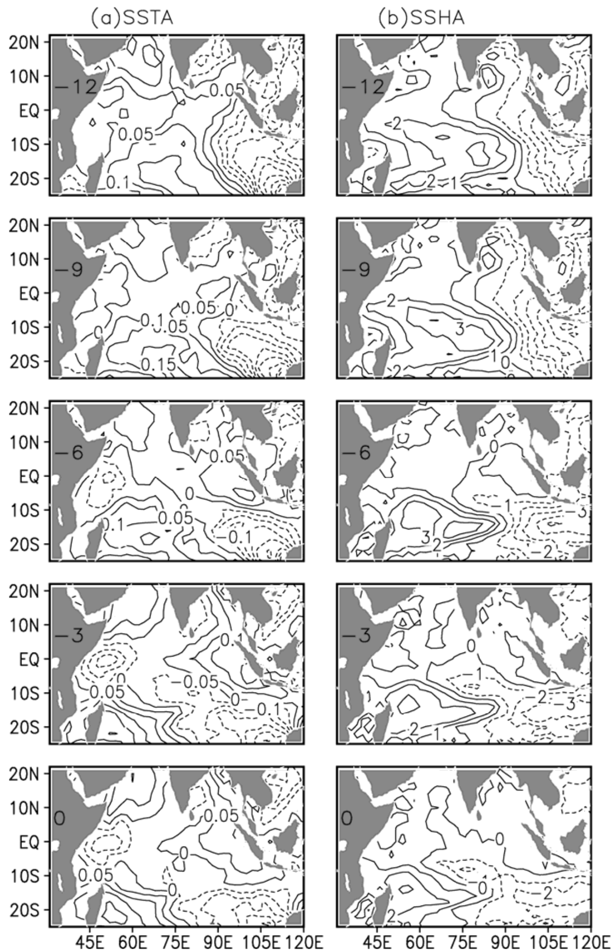


**Fig. 8.** Same as Fig. 7, but for time lags from minus 12 to zero months in reference to the sandwich mode.





OSD
9, 1–24, 2012

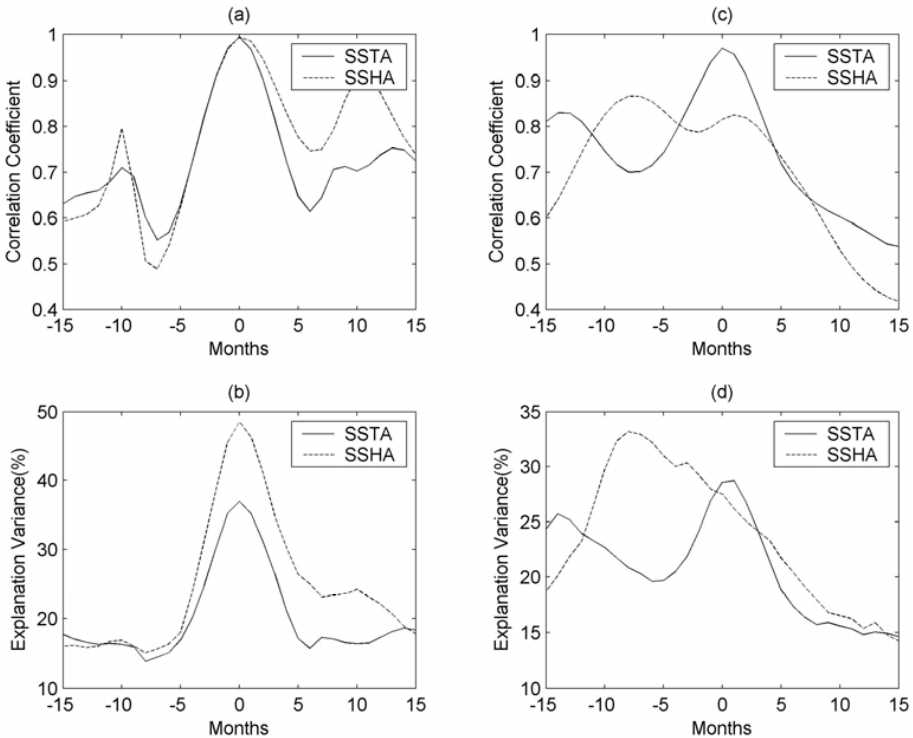


**Fig. 9.** **(a)** Correlation coefficients between the dipole mode and the associate mode and **(b)** variances explained by associate patterns for time leads from −15 to 15 months in reference to the dipole mode for SSTA (solid line) and SSHA (dashed line). **(c)** and **(d)** are same as **(a)** and **(b)**, respectively, but in reference to the sandwich mode.





OSD
9, 1–24, 2012

Interannual coherent variability of SSTA and SSHA in the Tropical Indian Ocean

J. Q. Feng